Food Bioprocess Technol
DOI 10.1007/s11947-016-1765-3

ORIGINAL PAPER

Effects of Exposure to Pulsed Light on Surface and Structural Properties of Edible Films Made from Cassava and Taro Starch

Tomy J. Gutiérrez[1,2] · **Gema González**[3]

Received: 6 March 2016 / Accepted: 22 June 2016

Abstract Edible films derived from starch have been proposed as packaging materials. However, they may suffer physicochemical changes due to a variety of factors, such as pulsed light (PL) treatments. In this study, the effect of PL treatment as a crosslinking method on films made from cassava (*Manihot esculenta* C.) and taro (*Colocasia esculenta* L. Schott) starch, plasticized with glycerol was evaluated. The average molecular weight, contact angle, moisture content, X-ray diffraction pattern, color, and mechanical and microstructural properties were evaluated. Films subjected to PL showed deterioration compared with control films as demonstrated by an increase in the contact angle, surface roughness, and crystallinity, and a decrease in the tensile strength, transparency, and water content, independent of the amylose content of the starches evaluated. Finally, the surface properties of these materials are defined by intermolecular interactions such as van der Waals-type force interactions (hydrogen bond), new bonds (crosslinking) formed between the biopolymeric chains (starch), and by breakage of covalent bonds.

Keywords Atomic force microscopy · Contact angle · Pulsed light · Starch · Surface

✉ Tomy J. Gutiérrez
tomy.gutierrez@ciens.ucv.ve; tomy_gutierrez@yahoo.es

[1] Departamento Químico Analítico, Facultad de Farmacia, Universidad Central de Venezuela, Apartado 40109, Caracas 1040-A, Venezuela

[2] Instituto de Ciencia y Tecnología de Alimentos, Facultad de Ciencias, Universidad Central de Venezuela, Apartado 47097, Caracas 1041-A, Venezuela

[3] Centro de Ingeniería de Materiales y Nanotecnología, Instituto Venezolano de Investigaciones Científicas, Apartado 20632, Caracas 1020-A, Venezuela

Introduction

The use of starch-based edible films as a substitute material for synthetic polymers has been the focus of extensive research in recent years (Gutiérrez et al. 2015a). Special emphasis has been placed on the preparation of edible films derived from cassava starch as a cheap, biodegradable, and innocuous material (Famá et al. 2005, 2006, 2007; Flores et al., 2007; Gutiérrez et al., 2015a, b). Nevertheless, these materials have several drawbacks associated to their hydrophilic properties (Al-Hassan and Norziah 2012). For this reason, different alternatives have been proposed to improve their properties; among them, we can mention the chemical and/or physical modifications of the starch (García-Tejeda et al. 2013). Most recently, Wihodo and Moraru (2015) have proposed the pulsed light (PL) as a modification method on biopolymeric films based on proteins. This method is based on the photo-induced polymerization, which uses light to initiate and propagate a polymerization reaction to form a crosslinked polymer structure (Wihodo and Moraru 2015).

It is worth noting that PL is a non-thermal emerging technology, which is based on ultraviolet (UV) radiation (Gómez-López et al. 2007; Krishnamurthy et al. 2010; Izquier and Gómez-López 2011). The use of PL for microbial inactivation has been reported quite extensively (Uesugi and Moraru 2009; Krishnamurthy et al. 2010; Cheigh et al. 2012), but Wihodo and Moraru (2015) have recently evaluated the potential of this technology for photo-polymerization applications. According to Wihodo and Moraru (2015), the broad spectrum of light and the high light intensity suggest that PL has a great potential to initiate efficient the photo-polymerization.

Published online: 07 July 2016

Photo-polymerization has been typically achieved by continuous UV radiation (Gennadios et al. 1998; Rhim et al. 1999; Vaz et al. 2003). Gennadios et al. (1998) reported that an UV dose of 51.8 J/m^2 increased the tensile strength of SPI films by 41.9 %. In another report, the same UV dose (51.8 J/m^2) increased the tensile strength of sodium caseinate films by 2.5 %, of egg albumin films by 70.6 %, of corn zein film by 20 %, and of wheat gluten films by 66.7 % (Rhim et al. 1999). Besides, many other studies have demonstrated that the physiochemical and mechanical properties of edible films may be modified by UV radiation (Ummi-Shafiqah et al. 2012; Otoni et al. 2012; Sionkowska and Płanecka 2013; Sionkowska et al. 2014).

However, authors such as Sionkowska et al. (2014) have recently observed that hydrocolloids may suffer a deterioration process caused by UV radiation. According to Cui et al. (2013), UV radiation is responsible for most aging damages, because the quantum energy of UV radiation is high enough to cause chain cleavage in the molecules, and this, in turn, resulting in one or more of the following chemical changes: depolymerization, crosslinking, and formation of double bonds in the polymer chain and other low-molecular compounds. These effects are usually classified as photo-degradation. Photo-degradation generally leads to an embrittlement of polymer materials and often causes a transition from ductile failure to brittle fracture. A reduction in yield stress, tensile stress, and elongation at break was observed in many photo-degraded materials (Fayolle et al. 2000; Turton and White 2001; Briassoulis et al. 2004; Ito and Nagai 2007).

Among the possible advantages of PL, as possible modification method of biopolymers, it can be mentioned: (1) Application time is in the order of seconds in changes other modifications even last for several hours, and (2) it can reduce the consumption of chemical reagents.

In this study, the microstructure, moisture content, and color were evaluated, as well as the mechanical and surface properties of edible films derived from cassava (*Manihot esculenta* C.) and taro (*Colocasia esculenta* L. Schott) starch in order to explore the possible use of PL as a photo-polymerization technique for improving the structural and mechanical properties of starch-based films.

Experimental

Materials

Taro (*C. esculenta* L. Schott) and cassava (*M. esculenta* C.) tubers were obtained from a local market in Caracas, Venezuela. The starch was extracted following the method described by Pérez et al. (1993) obtaining a yield of approximately 30 % in both cases (Gutiérrez et al. 2014). The total amylose content was determined by the differential scanning calorimetry (DSC) method described by Pérez et al. (2010, 2013). An approximate total amylose content of 15.1 % for the taro starch and 19.9 % for cassava starch was obtained. Dimethyl sulfoxide (DMSO) was purchased from Aldrich. Food-grade glycerol from Prolabo, Sweden, was used as a plasticizer for the formation of the films.

Film Formation

Films were prepared from a film-forming solution (FFS) made by mixing 4.5 % *w/v* of starch and 1.5 % *w/v* of glycerol in distilled water. The solutions were then heated in a water bath with constant shaking of 250 rpm at 98 °C for 30 min to ensure starch gelatinization (Hernández et al. 2008). Volumes of 15 mL were then poured onto plastic petri dishes (diameter 90 mm). The samples were then dried in a Mitchell dehydrator (Model 645,159) for 24 h at 48 °C. One group of dishes was exposed to PL and the other was used as control. Each group consisted of fifteen petri dishes to carry out all the characterizations in the same way. PL treatment was performed (on the experimental group) using a XeMaticA-1XL system (SteriBeam GmbH, Kehl, Germany) as described by Izquier and Gómez-López (2011), at the maximum fluence permitted by the Federal Drug Administration (FDA 2013) (12 J/cm^2). The method to expose the films to PL was as follows: each petri dish with the films developed was centered individually on an adjustable stainless steel shelf in the PL unit, at 5 cm beneath the Xenon lamp, and was treated with 8 light pulses. Likewise, the surface temperature of the films was maintained constant during the application of PL, this was verified by placing a thermocouple on the surface of the films exposed to PL. The resulting thermoplastic starch films: cassava control (*TPS-C*), cassava treated with pulsed light (*TPS-CPL*), taro control (*TPS-T*) and taro treated with pulsed light (*TPS-TPL*), were obtained. Before characterization, the films were conditioned at 57 % relative humidity (RH) for one week at 25 °C.

Characterization

Determination of Average Molecular Weight (M_w) of the Films Developed by the use of Ostwald Viscometer

Using DMSO as solvent, solutions at 1 % *w/v* of each film were assessed. Next, successive dilutions were prepared using different solutions at 0.125, 0.25 and 0.50 % *w/v*. Afterwards, the resistance time to the flow of the solutions prepared was determined, taking as reference the passage between two areas marked in Ostwald viscometer (Cannon-Fenske 200 series, model 120205, IVA, Argentina) at 25.0 ± 0.1 °C. After obtaining the residence time of the different solutions prepared, we proceeded to determine the relationship η_{exp}/C

through Eq. 1, which was empirically demonstrated by Kramer (1938) and Huggins (1942):

$$\eta_{exp}/C = {}^{1}/_{C} + {}^{t-t_o}/_{t_o} \quad (1)$$

where

η_{ex} $(\eta - \eta_o/\eta_o)$, intrinsic viscosity
η_o viscosity of the pure solvent
C concentration of the solutions % *w*/*v*
t residence time of the solutions
t_o residence time of the pure solvent

Using Eq. 2:

$$\eta_{exp}/C = \eta + KC\eta^2 \quad (2)$$

and graphing η_{exp}/C vs C, a straight of cut point equal to η was obtained. At the same time, using the Mark-Houwink-Sakurada-Staudinger equation (Eq. 3):

$$\eta = \mathrm{K}M_w{}^{a} \quad (3)$$

where

η intrinsic viscosity
M_w polymer molecular weight
K and ^{a} constants reported for the solvent used (DMSO)
K 0.0112 mL/g at 25 °C
^{a} 0.72 at 25 °C

Finally, the average molecular weight (M_w) of the films tested was calculated from Eq. 4:

$$M_w = \left({}^{\eta}/_{K}\right)^{1/a} \quad (4)$$

Moisture Content

The moisture content of the different systems was determined by a gravimetric method according to Rhim and Wang (2013), with some modifications and using the following equation:

$$\%\text{moisture} = \frac{m_w - m_d}{m_w} \times 100 \quad (5)$$

where m_w is the wet mass and m_d the dry mass of the film systems.

The protocol used is based on the method of analysis according to the International Association of Official Analytical Chemistry (AOAC 1990).

For this, the dry mass was determined by heating a ~0.5 g sample of each film in an oven at 100 °C for 24 h. An analytical balance (Denver Instrument APX-200) was used to monitor the weight. Analyses were performed in triplicate, and the average percentage of moisture was reported.

X-ray Diffraction

X-ray diffraction tests on the different films were performed using a vertical goniometer X-ray diffractometer (Siemens D 5000) (radiation Cu αK = 1.5406 Å, 40 kV, and 30 mÅ). Scattered radiation was detected in an angular range of 3°–33° (2θ) at a step size of 0.02° and scan speed of 2 s. The distances between the planes of the crystals d (Å) were calculated from the diffraction angles (°) measured from the X-ray pattern, according to Bragg's law:

$$n\lambda = 2d\sin(\theta) \quad (6)$$

where λ is the wavelength of radiation Cu αK and n is the order of reflection. For the calculations, n was taken as 1. The thicknesses of the samples on the slides were ~200 μm. Percent crystallinity was determined by measuring the relative intensity of the main peaks from the scattering spectrum according to Hermans and Weidinger (1961).

Scanning Electron Microscopy

Films were cryofractured by immersion in liquid nitrogen, mounted on bronze stubs, and sputter coated with a thin layer of gold for 35 s. The fracture surface of each material was then analyzed using a Philips XL series 30 (Holanda) scanning electron microscopy.

Uniaxial Tensile Strength

At least 15 pieces of each film, with effective length 12 mm and width 0.5 mm, were cut and evaluated. Tests were performed at ambient temperature (25 °C) with an Instron dynamometer (Instron Ltd., High Wycombe, UK) (5 lbs) at 0.02 in/s, according to ISO 527-2 (2012). The stress-strain behavior of the films was calculated from the force-time curves. Young's modulus (E), maximum stress (σ_m), strain at break (ε_b), and toughness (T) were reported. Calculations were done following Gutiérrez et al. (2015a).

Color

The color parameters of the films, L^*, a^*, and b^*, were measured according to the standard test method (ASTM D-1925, 1995) using a Macbeth® colorimeter in mode reflectance (Color-Eye 2445 model, illuminant D65 and 10° observer) standardized with a white reference plate ($L^* = 93.52$, $a^* = -0.81$, and $b^* = 1.58$). Color differences (ΔE) were calculated according to Medina

et al. (2015) and the yellowness index (YI), according to ASTM D-1925 (MacFarlane et al. 1936) using the CIELAB scale.

Atomic Force Microscopy

Agilent 5500 atomic force microscope in the acoustic AC mode (AAC mode) with silicon nitride (Si_3N_4) tips was used to take the topographic images of the films obtained. The surface analyzed was the side of the surface exposed to the drying air during film preparation. Likewise, this was also the surface exposed to PL. Moreover, Si_3N_4 tips had a spring constant of 0.2 N/m and a V-shaped tip 2 mm long, which was positioned over the sample under ambient conditions. The atomic force microscopy (AFM) images were taken at the center and periphery of the surface of the films. The AFM images were processed with PicoView image software.

Contact Angle

An USB digital microscope (model DIGMIC200X, China) equipped with Image Analysis Software 220X 2.0MP video, with 0.01° precision was used for determining the contact angle. A drop of distilled water (2 μL) was placed on the surface exposed to the drying air during film preparation of each material. The contact angles (θ) were calculated by analyzing the images to determine the angles formed by the intersection of the liquid-solid interface (drop of water-surface of the film) and the liquid-vapor interface (tangent to the boundary of the drop) (Karbowiak et al. 2006). A total of 12 contact angles were measured per film.

The contact angles were determined at a temperature of 25 °C and measured on the side of the surface exposed to the drying air during film preparation. Likewise, this was also the surface exposed to PL. Measurements were taken just at the moment when the drop of water came into contact with the film surface. This was done in order to avoid false results caused by phenomena such as dehydration, swelling, and dissolution (Vogler et al. 1995).

Statistical Analysis

The analysis of data was performed through the analysis of variance (ANOVA) using the Statgraphics Plus 5.1. software (ManugisticsCorp., Rockville, MD). Fisher's least significant difference (LSD) procedure was used at the 95 % confidence level.

Results and Discussion

Average Molecular Weight of the Films Developed

Table 1 shows the molecular weight of the different films studied. Films with highest molecular weight were obtained for taro films (TPS-T and TPS-TPL). This is consistent with the results reported by Yoo and Jane (2002) for starches with lowest amylose values. A slight increase in molecular weight of the taro starch film exposed to PL (TPS-TPL) was observed, which could be related to crosslinking of the taro starch, though this was not statistically significant. In contrast, a significant decrease in molecular weight of the cassava starch film exposed to PL (TPS-CPL) was observed, suggesting depolymerization of amylose chains due to PL treatment.

Moisture Content

Table 1 shows the moisture content of the different films studied. The films made from taro starch (TPS-T and TPS-TPL) had a higher moisture content than cassava-based films. According to previous studies (Flores et al. 2007; Hu et al. 2009; Gutiérrez et al. 2015a), amylopectin-glycerol interactions in plasticized starch-based films are weaker than

Table 1 Molecular weight, moisture content, crystallinity, contact angle, and color parameters of the different films

Parameter	TPS-C	TPS-CPL	TPS-T	TPS-TPL
Average molecular weight ($\times 10^8$ g/mol)	1.3 ± 0.2^{b}	0.7 ± 0.1^{a}	12.6 ± 0.3^{c}	13.1 ± 0.2^{c}
Moisture (%)	20 ± 1^{b}	17 ± 1^{a}	29 ± 1^{d}	26 ± 1^{c}
Crystallinity (%)	19.0 ± 0.2^{c}	21.0 ± 0.2^{d}	10.0 ± 0.1^{a}	11.0 ± 0.1^{b}
Contact angle (deg)	59 ± 1^{c}	62 ± 1^{d}	43 ± 2^{a}	53 ± 2^{b}
L^*	16.1 ± 0.3^{c}	17.4 ± 0.2^{d}	7.33 ± 0.03^{a}	12.65 ± 0.09^{b}
a^*	-0.5 ± 0.1^{a}	-0.33 ± 0.05^{b}	-0.13 ± 0.05^{c}	-0.12 ± 0.06^{c}
b^*	-0.71 ± 0.02^{c}	-0.99 ± 0.08^{b}	-1.39 ± 0.04^{a}	-0.8 ± 0.1^{c}
Color difference (ΔE)	75 ± 3^{a}	76.2 ± 0.2^{a}	86.26 ± 0.02^{c}	80.93 ± 0.09^{b}
Whiteness index (WI)	16.1 ± 0.3^{c}	17.4 ± 0.2^{d}	7.32 ± 0.02^{a}	12.64 ± 0.09^{b}
Yellowness index (YI)	$-5.6 \pm 0.2^{b,c}$	-7.3 ± 0.4^{b}	-14.1 ± 0.5^{a}	-6.6 ± 0.9^{b}

Equal letters in the same row indicate no statistically significant differences ($p \leq 0.05$). Thermoplastic starch films: cassava control (*TPS-C*), cassava treated with pulsed light (*TPS-CPL*), taro control (*TPS-T*) and taro treated with pulsed light (*TPS-TPL*)

glycerol-amylose interactions. Taro starch contains a lower percentage of amylose than cassava starch (15.1 and 19.9 %, respectively), and weak amylopectin-glycerol interactions facilitate water absorption (Flores et al. 2007; Hu et al. 2009; Gutiérrez et al. 2015a). This explains the higher moisture content in taro starch films. This phenomenon is commonly known as moisture plasticization because the weak starch-glycerol interaction water can act as a plasticizer. Gutiérrez et al. (2015a, b) reported this type of behavior in a recent paper on waxy cushcush yam starch films. As previously mentioned, glycerol interacts more strongly with cassava starch as compared to taro starch probably due to the formation of hydrogen bonds between the glycerol and the amylose. The glycerol-amylose interactions lead to a reduction in the intra- and intermolecular interactions between the starch macromolecules, thus increasing the movement and rearrangement of the chains.

The application of PL on the films tended to decrease significantly ($p \leq 0.05$) the moisture content of the materials. This tendency is possibly due to the crosslinking caused by UV radiation on the films treated with PL (Merlin and Fouassier 1981; Andrady et al. 1998; Cui et al. 2013).

X-ray Diffraction

Figure 1 shows the X-ray diffraction patterns of the developed films. The diffraction curves of all the films studied show a behavior typical of a semicrystalline material mainly composed of an amorphous phase with a small crystalline fraction. This is consistent with that reported in the literature for starch-based films (Angellier et al. 2006; Famá et al. 2006, 2007, 2005; Flores et al. 2007; Kristo and Biliaderis 2007; García et al. 2009; Gutiérrez et al. 2015b, c).

In general, starches show A-, B-, and C-type crystal structures. When glycerol is present, the double helix conformations are disrupted by the formation of stable single chain V-conformation helices resulting in the glycerol-amylose complex (Zobel 1994; Farhat et al. 1999; Manzocco et al. 2003). As can be seen in Fig. 1a, the cassava starch films showed curves with diffraction peaks corresponding to the following *d*-spacings ≅ 3.6, 3.8, 4.1, 4.5, 4.8, 5.0, 5.9, and 8.8 Å, associated with A-type structures. Peaks corresponding to the *d*-spacings ≅ 4.1, 5.0, and 14.7 Å, associated with B-type structures, were also observed (Famá et al. 2005; García et al. 2009; Gutiérrez et al. 2015b) as were peaks with *d*-spacings ≅ 4.5 and 6.8 Å associated with V-type structures (Zobel et al. 1967). As regards the taro starch films (Fig. 1b), these developed discrete conformations of A-type structures, with peaks corresponding to *d*-spacings ≅ 3.8, 4.1, 4.5, 5.2, 6.1, and 7.8 Å. Peaks corresponding to *d*-spacings ≅ 4.1 and 5.2 Å were associated with B-type structures. According to García-Tejeda et al. (2013), the signal observed for 2 = 17.2, corresponding to *d*-spacing ≅ 5.2 Å, is associated with interactions between the short external amylopectin chains and glycerol.

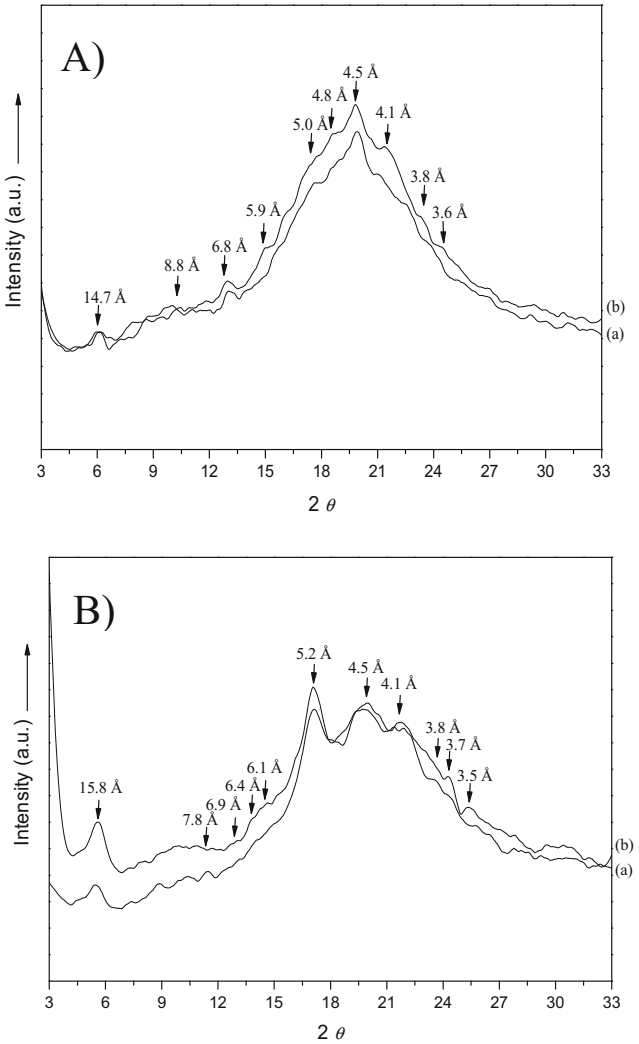

Fig. 1 X-ray diffraction pattern of the different films studied: **a** (*a*) cassava control (TPS-C), (*b*) cassava treated with pulsed light (TPS-CPL), and **b** (*a*) taro control (TPS-T) and (*b*) taro treated with pulsed light (TPS-TPL)

Similarly, the peaks with *d*-spacings ≅ 4.5, 6.4, and 6.9 Å observed in the taro starch films correspond to a V-type structure. García et al. (2009) observed the same behavior in waxy starch films with peaks corresponding to *d* ≅ 3.9, 5.1, and 5.9 Å, and similar results have also been reported by Primo-Martin et al. (2007) and Thielemans et al. (2006).

The A-type patterns observed in TPS-T and TPS-TPL may be due to a local order generated by associated amylopectin chains. According to the literature, the crystallinity of starch films is mainly associated with the amylose contained within the branches of the amylopectin (Zobel, 1992). In Fig. 1a, it can be observed that the areas under the crystallinity peaks are larger in cassava starch films than taro starch films (Fig. 1b). This behavior is expected, as cassava starch contains more amylose than taro starch.

Furthermore, the crystallinity of the films exposed to PL (TPS-CPL and TPS-TPL, Fig. 1a (b), b (b), respectively)

slightly increased. The values of the crystallinity percentages, calculated from the surface area under the curves, confirmed this (Table 1). This can also be observed, since the areas under the crystallinity peaks are larger in films exposed to PL compared to the control films. Similar results were reported by Ummi-Shafiqah et al. (2012) who evaluated the properties of glycerol-plasticized films made from sago and mung beans, prepared by casting and exposed to UV radiation during 2 h. This effect maybe produced by the retrogradation of starch during aging or by deterioration process, which reduces chain mobility (Bertuzzi et al. 2007; García-Tejeda et al. 2013). This behavior provides further evidence that exposure to PL produced a deterioration effect in the evaluated films.

According to Osella et al. (2005), the development of A- or B-type X-ray diffraction patterns in starch films also depends on their water content. A decrease in moisture is highly correlated with an increase in the crystal phase of a semicrystalline material (Chang et al. 2000; Famá et al. 2005; Hu et al. 2009; Pelissari et al. 2013). Thus, the slight increase observed in the crystallinity of cassava starch films (Fig. 1a) correlates with the lower humidity values obtained for these materials (García et al. 2000). Similar behavior was observed in the films exposed to PL.

Scanning Electron Microscopy

Figure 2 shows the scanning electron microscopy (SEM) images of the cryofractured surfaces of the different films. It can be seen that the films produced are non-porous. All the systems presented a compact structure, but this was far more marked in the films made from cassava starch (Fig. 2a, b). Similar structures have been reported by Saavedra and Algecira (2010) for cassava starch-protein films. Also, García et al. (2009) and Gutiérrez et al. (2015a) obtained

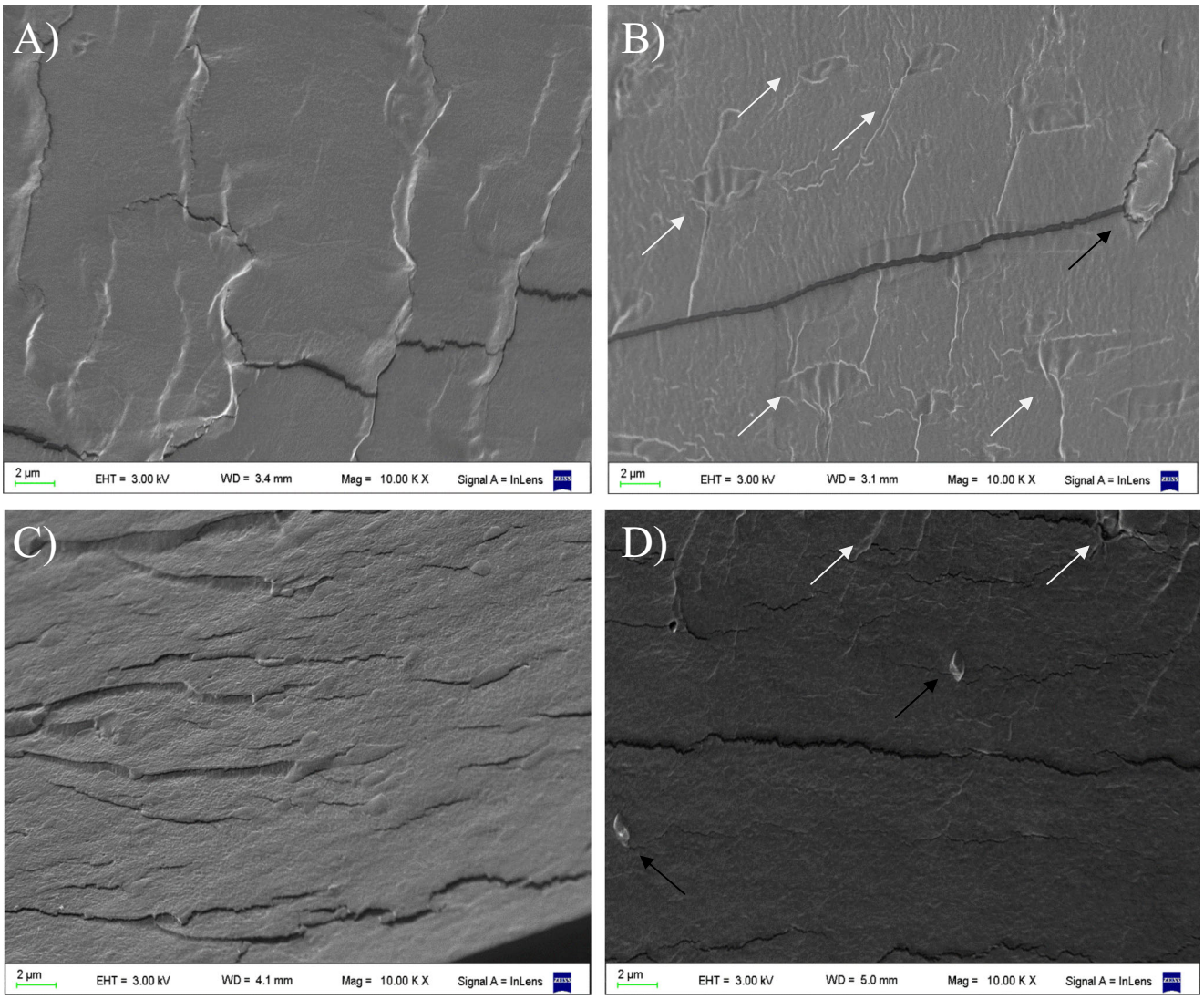

Fig. 2 SEM micrographs of the cryogenic fractured surface of the films: **a** cassava control (TPS-C), **b** cassava treated with pulsed light (TPS-CPL), **c** taro control (TPS-T) and **d** taro treated with pulsed light (TPS-TPL). At ×10k of magnification. *Black lines* indicate granules and *white lines*, creases

similar structures in their study of cassava-glycerol films. This is probably produced by the high amount of amylose present in cassava starch systems (Miles et al. 1985a, b; Noel et al. 1992). Following Pelissari et al. (2013), a more compact structure leads to lower water adsorption as it makes interactions between the starch-glycerol and water less likely, leading to a decrease in the polar glycerol-starch character of the films (García-Tejeda et al. 2013). The moisture content results obtained for the starch-based systems analyzed (Table 1) agree with the structures observed by SEM.

The films treated with PL showed a more compact structure than the controls, indicating a lower water absorption capacity. This result correlates with the tendency towards a lower moisture content reported for these materials.

In addition, small crystals were observed in the TPS-CPL and TPS-TPL samples. These were more developed on the cassava starch-based films possibly due to the recrystallization of the starch caused by the deterioration process generated by the PL treatment. The presence of these crystals in TPS-CPL and TPS-TPL samples is consistent with the slight increase in the crystallinity of these films and the X-ray diffraction results.

Besides, the films treated with PL showed wrinkles typical of materials aged by UV radiation (Sionkowska et al. 2014). The density of these wrinkles was higher for the cassava starch films. This agrees with that observed by Ummi-Shafiqah et al. (2012) who indicated that UV radiation produces starch photo-degradation resulting in the cleavage of glycosidic bonds accompanied by the shortening of the amylose and a debranching of the amylopectin chains due to the formation of free radicals (Merlin and Fouassier 1981). Thus, it seems that the wrinkles observed in the films exposed to PL are characteristic of an additional effect produced by starch photo-degradation (Ummi-Shafiqah et al. 2012; Cui et al. 2013; Sionkowska et al. 2014).

Uniaxial Tensile Strength

The stress-strain curves of each film system studied are shown in Fig. 3. A small linear zone was observed followed by a nonlinear zone until breaking point, regardless of the starch used. A more pronounced brittle behavior was found for taro starch films, which fell sharply immediately after breaking point. Table 2 shows the values of the mechanical parameters for the four film systems. The starches evaluated differed markedly, both in their maximum stress and strain at break values, without the elastic modulus being significantly modified. As can be observed, the stress necessary to break the cassava starch-based films was twice that needed to break the taro starch films and the deformation capacity of the former was also five times greater. It is well known that the mechanical properties of edible films are highly influenced by the amylose-amylopectin ratio. An increase in the concentrations of amylose leads to an increase in the strain at break (Famá et al. 2015). However, simultaneous increases in the stress and deformation parameters have not been often reported. Li et al. (2011) observed this behavior when he compared maize films (20 % amylose) with films made from waxy materials (4.3 % amylose) without obtaining significant changes in the E' modulus.

The greater deformation capacity of the cassava-based films could be explained by the observations of the X-ray diffraction assays. As we observed from the analysis of the curves in Fig. 1, the peak with the highest intensity located at

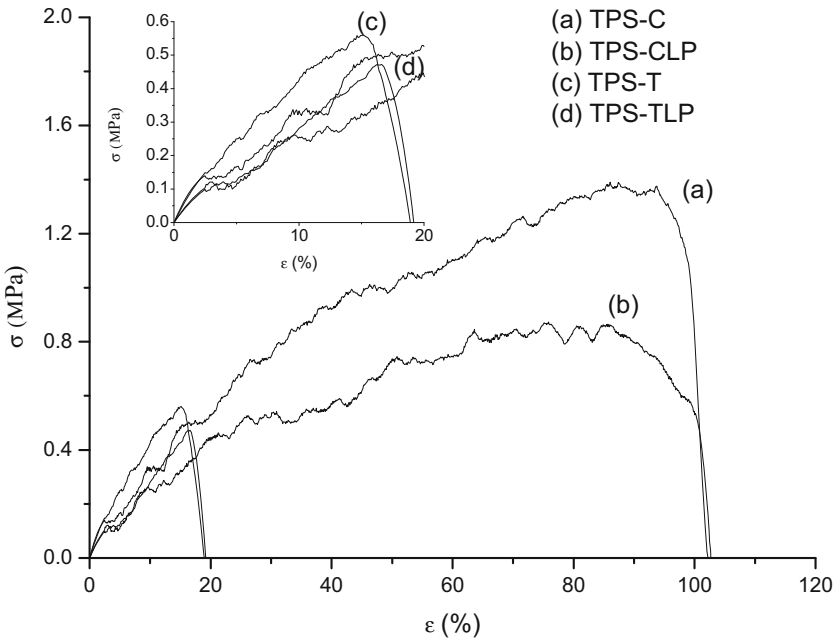

Fig. 3 Stress (σ)–strain (ε) curves of the films: *a* cassava control (TPS-C), *b* cassava treated with pulsed light (TPS-CPL), *c* taro control (TPS-T) and *d* taro treated with pulsed light (TPS-TPL)

Table 2 Parameters of the uniaxial tensile tests: Young's modulus (E), maximum stress (σ_m), strain at break (ε_b), and tenacity (T) of the different films

Material	E (MPa)	σ_m (MPa)	ε_b (%)	T ($\times 10^3$) (J/m^3)
TPS-C	3.4 ± 0.2^b	1.3 ± 0.1^c	104 ± 1^b	95.0 ± 0.1^c
TPS-CPL	2.3 ± 0.6^a	1.0 ± 0.1^b	105 ± 5^b	62.2 ± 0.5^b
TPS-T	5.1 ± 0.9^b	0.58 ± 0.06^a	18.2 ± 0.8^a	6.3 ± 0.8^a
TPS-TPL	5.2 ± 0.4^b	0.51 ± 0.05^a	20 ± 2^a	4.8 ± 0.7^a

Equal letters in the same column indicate no statistically significant difference ($p \leq 0.05$). Thermoplastic starch films: cassava control (*TPS-C*), cassava treated with pulsed light (*TPS-CPL*), taro control (*TPS-T*), and taro treated with pulsed light (*TPS-TPL*)

~4.5 Å is associated with a high degree of hydrogen bonding. This indicates that the glycerol interacts more strongly with cassava than with taro starch, probably due to the formation of hydrogen bonds between the glycerol and the amylose molecules (Gutiérrez et al. 2015a). The glycerol-amylose interaction weakens the intra- and intermolecular interactions between starch macromolecules. This leads to an increase in the movement and rearrangement of their chains, and thus in the flexibility of TPS-C and TPS-CPL, resulting in an increase in their strain at break values (Hu et al. 2009).

In addition, a stronger glycerol-amylose interaction limits the possible interaction between water and glycerol or starch, thus decreasing the moisture levels in the cassava starch films (Table 1).

Different authors have related the elasticity of cassava starch films with their structure, indicating that higher elasticity values are associated with materials with a more compact structure (Saavedra and Algecira 2010; Gutiérrez et al. 2015a). This agrees with our results where films with greater degree of compactness (Fig. 2a, b) were also more elastic.

It is worth noting that the high values of the stress and strain at break parameters for the cassava starch films were correlated with the high tenacity of these materials. This means that food packaging made from cassava starch would show a greater resistance against knocks and bumps. It is also worth mentioning that the high deformation capacity of this material means that it could also be very appropriate for other types of packaging especially bags.

Samples treated with PL showed a reduction in Young's modulus and maximum stress values, this probably owing to a lowering of their mean molecular weight associated with photo-chemical degradation (Sionkowska et al. 2014; Wihodo and Moraru 2015). This agrees with the SEM images and the molecular weight obtained (Fig. 2b, d). Similar results were reported by Sionkowska et al. (2014) for films made from chitosan. Another possible reaction caused by photodegradation is reticulation that would also lead to a decrease in Young's modulus. Similar results were reported by Gutiérrez et al. (2015a, c) for films derived from cassava, maize, and cush-cush yam starches crosslinked with sodium trimetaphosphate.

Furthermore, crystalline particles often act as nuclei for inducing the recrystallization (retrogradation) of starch macromolecules (Mina et al. 2009) leading to less resistant materials (García et al. 2009). This agrees with our data (Fig. 2b, d) as the tensile strength of the cassava starch films significantly decreased compared to the taro starch films when treated with PL. This fits in well with the chemical composition of the starches as the amylose in the TPS-CPL develops larger crystals making it more prone to retrogradation and concurs with that reported by Cui et al. (2013) and Sionkowska et al. (2014) for thermoplastic materials derived from dicyclopentadiene and chitosan, respectively.

Treatment with PL did not significantly modify the strain at break of either of the films evaluated (Table 2) (TPS-CPL and TPS-TPL). Similar results were reported by Wihodo and Moraru (2015); although to higher fluence (23.5 J/cm^2 exceeds the maximum fluence permitted by the FDA), they found an increase of strain at break in films based on proteins. According to Wihodo and Moraru (2015), this suggests some degree of crosslinking and the formation of a slightly more ductile network after PL treatments, since the formation of covalent bonds will allow the network to deform more before reaching the breaking point.

The toughness values were lower for the films made from taro starch, in agreement with that reported by Gutiérrez et al. (2015a) for films with a low amylose content. Similarly, TPS-CPL showed lower toughness values than TPS-C due to marked differences in their tensile strengths, as explained above. Cui et al. (2013) reported similar results for films derived from dicyclopentadiene.

The mechanical properties of both types of film show that they could both be considered as coatings depending on the particular requirements of the product to be coated. Taro starch based materials are recommended for coverings where a certain degree of resistance is needed and cassava starch based films for more flexible coatings.

Color

Table 1 shows the results of the color parameters of the films studied. The values of the L^* index and whiteness index (WI) were higher for the cassava starch films (TPS-C and TPS-CPL) than for films made from taro starch (TPS-T and TPS-TPL). Thus, the cassava starch films were whiter and more opaque than the taro starch films. These results are similar to those reported by Gutiérrez et al. (2015a) and confirm that films with a lower amylose content are more transparent. According to the luminosity values obtained, the stronger interactions between the starch and the plasticizer (glycerol) produce more opaque films (Gutiérrez et al. 2015c). Fakhouri et al. (2007) indicate that opacity can vary in

function of the amylose content of starch as well as of molecules in solution, since their linearity tends to align themselves in parallel, close enough to form hydrogen bonds between the hydroxyl groups of adjacent chains. As a result, the affinity of polymer by water decreases favoring the formation of opaque pastes and flexible films, which correlates with the rest of the results obtained. Despite the differences in L^* and WI between the films, it is important to note that both materials showed excellent transparency and would thus be acceptable to customers. The more opaque TPS-C and TPS-CPL films could be more appropriate when protection against incident light is necessary, especially for wrapping products that are sensitive to degradation reactions catalyzed by light (Pelissari et al. 2013). In contrast, the more transparent films (TPS-T and

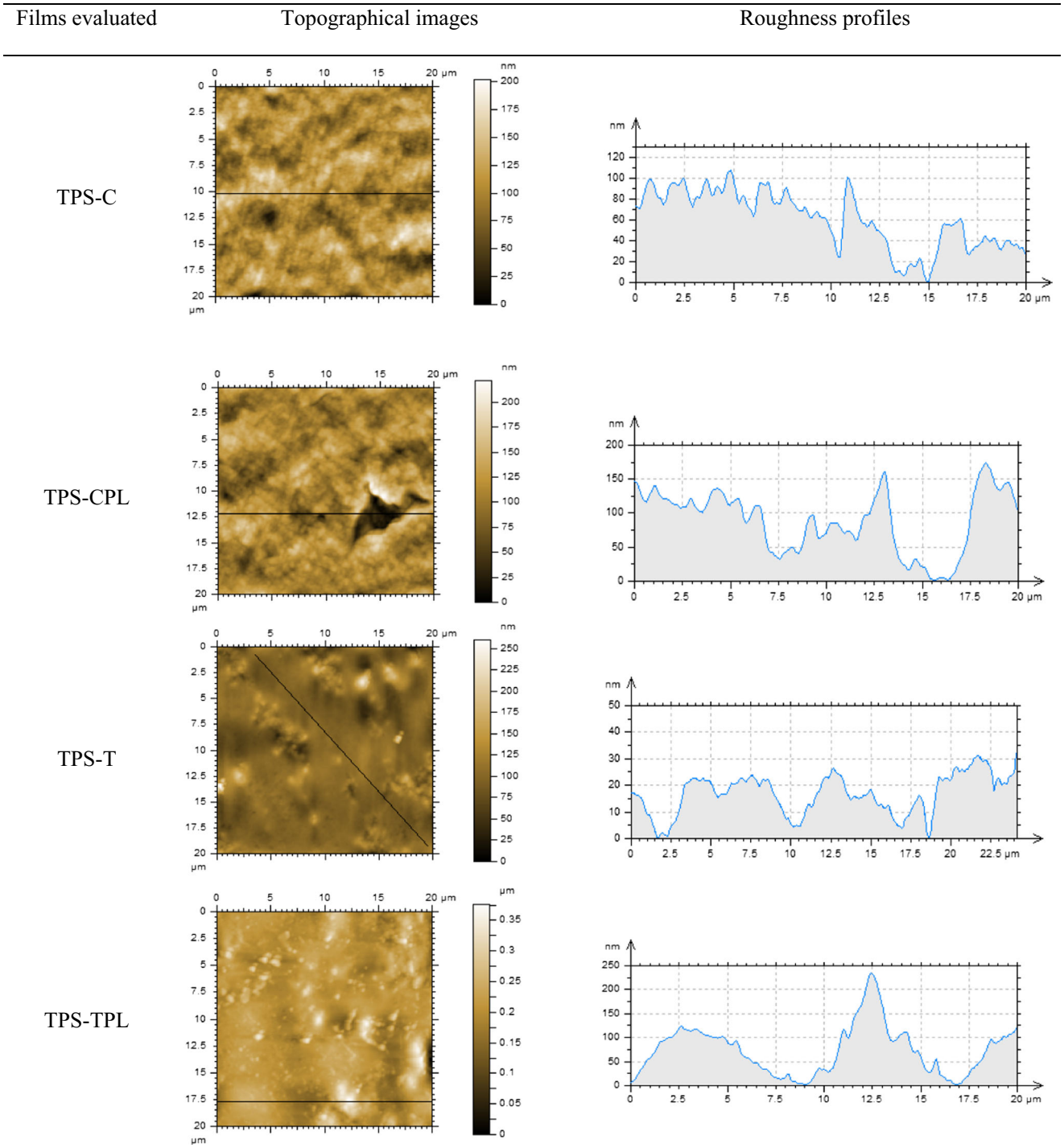

Fig. 4 AFM images of the films: cassava control (*TPS-C*), cassava treated with pulsed light (*TPS-CPL*), taro control (*TPS-T*), and taro treated with pulsed light (*TPS-TPL*)

TPS-TPL) could be particularly useful for foods that benefit from being seen through their wrappings to attract consumers (Gontard et al. 1992). PL also significantly increased ($p \leq 0.05$) the opacity of both starch films, demonstrating that PL causes an increase in hydrogen bond interactions between the starch and the glycerol, possibly due to crosslinking caused by UV radiation. This agrees with that reported by Gutiérrez et al. (2015a, c) for starches crosslinked with sodium trimetaphosphate. All this is consistent with the results of the mechanical properties of the films.

All the samples evaluated showed a^* values of around zero; however, the cassava starch films showed more negative values, indicating a tendency towards green in the systems with a higher amylose content. In contrast, the films treated with PL showed a slight tendency away from green. This may be due to the oxidation of pigments associated with starch.

A negative b^* value indicates a tendency towards blue. All the films studied showed this tendency.

The combination of all the changes observed in the chromatographic parameters L^*, a^*, and b^* produced slightly greater changes in color, ΔE, in the taro starch films. The results of the yellowness index (YI) were consistent with b^*, being negative in all cases, indicating a very low degree of yellowing of all the materials evaluated.

Topography of the Edible Films as Assessed by Atomic Force Microscopy

The topography and roughness profiles of the edible films assessed by AFM are shown in Fig. 4. Films made from cassava starch (with a higher amylose content) showed greater surface roughness than those made from taro starch. This behavior is consistent with the luminosity results obtained. Reyes (2013) mentions that films with a high roughness profile are more opaque, i.e., less transparent. This is probably due to the fact that a rougher surface texture does not permit the reflection of light which is thus absorbed by the film. This effect was also heightened after treatment with PL.

Contact Angle

Table 1 shows the measurements of the contact angles of the films studied. Cassava starch films showed higher contact angle values. It is well known that the contact angle of water increases with an increase in surface hydrophobicity (Ojagh et al. 2010). Karbowiak et al. (2006) suggested that an increase in the water contact angle of biopolymers could be due to strong intermolecular hydrogen bonding under the film surface. This means that the more polar sites (Lewis sites) would be affected, thus generating a reduction in the surface polarity of biopolymer films. Thus, the surface of the cassava starch films is dryer because it does not contain enough energy to break the cohesive force of water (Vogler 1998).

Figure 5 shows that the surfaces of the cassava starch films are more hydrophobic that those of the taro starch films. This correlates with the SEM images (Fig. 2b) in that Vogler (1998) indicates that a hydrophobic surface requires Lewis sites in order for the humidity to increase. The cassava starch films (with a higher amylose content) have a closed structure that acts as a physical barrier to water.

Interestingly, this kind of water structure requires that the hydrogen bond network of water directly adjacent to a nonpolar surface is interrupted, yielding "dangling hydrogen bonds." These dangling hydrogen bonds have been theoretically predicted (Lee et al. 1984) and spectroscopically resolved from hydrogen bonds in bulk water (Du et al. 1993, 1994a, b). An increase in the contact angle between the surface and water would generate dangling hydrogen bonds in the cassava starch films. The lower contact angle values of the taro starch films were due to the weak interactions favoring

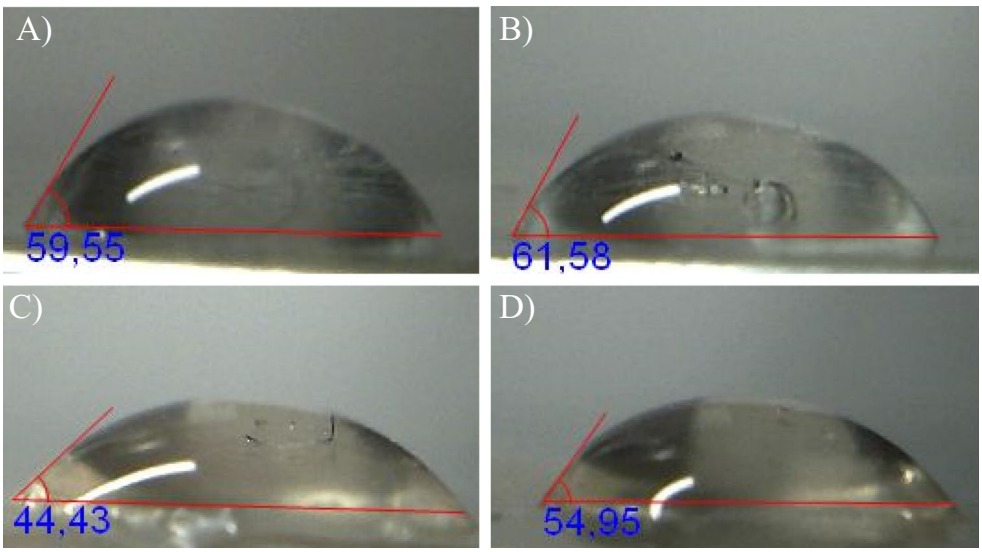

Fig. 5 Contact angle of the films: **a** cassava control (TPS-C), **b** cassava treated with pulsed light (TPS-CPL), **c** taro control (TPS-T), and **d** taro treated with pulsed light (TPS-TPL)

phase separation between the taro starch (higher amylopectin content) and the glycerol (Famá et al. 2006, 2007) leading to an increase in the density of Lewis sites on the surface. The Lewis sites on the taro starch films would come close to the hydrogen bond network in water, thus competing with cohesive forces and leading to the collapse of the water structure on a hydrophilic surface with a corresponding decrease in the contact angle. This is why films with a higher amylopectin content have sticky surfaces.

The deterioration effect on the films caused by PL produced a slight increase in the strength of the hydrogen bonds leading to a reduction in the number of Lewis sites. This could be appreciated by the fact that the contact angle increased in the treated films. Nevertheless, this effect was not so apparent in the cassava starch films compared with the taro starch-based films. This possibly was owing to higher amylose content in cassava starch since as it is known, amylose tends to form stronger hydrogen bonds with the glycerol (Gutiérrez et al. 2015a).

Surface roughness is another phenomenon that can be explained by an increase in the contact area and is strongly related to the molecular re-organization of the polymer matrix (Karbowiak et al. 2006). In the cassava starch films (higher amylose content), hydrogen bonding acts in opposition to retrogradation. This creates twisting forces in the starch macromolecules generating crater-like holes in the surface. The holes increase the surface roughness of the films (Fig. 4, TPS-C and TPS-CPL) by creating physical obstacles, which in turn lead to less surface moisture, thus increasing the contact angle.

Conclusions

We prepared edible films from cassava and taro starch plasticized with glycerol. The edible films with a higher amylose content (cassava) had greater contact angles and were rougher, more opaque, elastic, and dryer than the taro film systems. This was due to the formation of stronger hydrogen bond interactions between the starch and the glycerol. This hypothesis was confirmed by SEM images which showed that the cryofractured surface of the cassava starch films had a more closed structure, leading to a decrease in the density of Lewis sites on the surface of the films and modifications to their hydrophilic characteristics. On the other hand, the films that were subjected to PL treatment showed more closed structures independently of their amylose content. Edible films treated with PL suggest the modification by crosslinking. But nevertheless, apparently, the photo-degradation reaction dominates the reaction mechanism compared to the photo-polymerization reaction (crosslinking), according to the conditions of maximum fluence permitted by the FDA (12 J/cm^2). This was evident from the deterioration of mechanical properties and surface characteristics of the systems evaluated. Likewise, this was independent of amylose content of the starches evaluated.

Acknowledgments The author would like to thank the Fondo Nacional de Ciencia y Tecnología (FONACYT) of the Bolivarian Republic of Venezuela for co-financing this research project (grant S3-2012002114), M.Sc. Adriana Izquier, Dr. María Soledad Tapia, Dr. Lucía Famá and Dr. Mirian Carmona-Rodríguez.

References

Al-Hassan, A. A., & Norziah, M. H. (2012). Starch-gelatin edible films: water vapor permeability and mechanical properties as affected by plasticizers. *Food Hydrocolloids, 26*(1), 108–117.

Andrady, A. L., Hamid, S. H., Hu, X., & Torikai, A. (1998). Effects of increased solar ultraviolet radiation on materials. *Journal of Photochemistry and Photobiology B: Biology, 46*, 96–103.

Angellier, H., Molina-Boisseau, S., Dole, P., & Dufresne, A. (2006). Thermoplastic starch-waxy maize starch nanocrystals nanocomposites. *Biomacromolecules, 7*, 531–539.

Association of Official Analytical Chemists (AOAC). (1990). *Official methods of analysis*. 13th ed., Washington, DC.

ASTM D-1925 (1995). *Standard test method for yellowness index of plastics*. Philadelphia: American Society for Testing and Materials.

Bertuzzi, M. A., Castro, E. F., Armada, M., & Gottifredi, J. G. (2007). Water vapor permeability of edible starch based films. *Journal of Food Engineering, 80*(3), 972–978.

Briassoulis, D., Aristopoulou, A., Bonora, M., & Verlodt, I. (2004). Degradation characterisation of agricultural low-density polyethylene films. *Biosystems Engineering, 88*(2), 131–143.

Chang, P., Chea, P. B., & Seow, C. C. (2000). Plasticizing–antiplasticizing effects of water on physical properties of cassava starch films in the glassy state. *Journal of Food Science, 65*(3), 445–451.

Cheigh, C. I., Park, M. H., Chung, M. S., Shin, J. K., & Park, Y.-S. (2012). Comparison of intense PL and UV (UVC) induced cell damage in *Listeria monocytogenes* and *Escherichia coli* O157:H7. *Food Control, 25*, 654–659.

Cui, H., Hanus, R., & Kessler, M. R. (2013). Degradation of ROMP-based bio-renewable polymers by UV radiation. *Polymer Degradation and Stability, 98*, 2357–2365.

Du, Q., Freysz, E., & Shen, Y. R. (1994a). Surface vibrational spectroscopic studies of hydrogen bonding and hydrophobicity. *Science, 264*(5160), 826–828.

Du, Q., Freysz, E., & Shen, Y. R. (1994b). Vibrational spectra of water molecules at quartz/water interfaces. *Physical Review Letters, 72*(2), 238.

Du, Q., Superfine, R., Freysz, E., & Shen, Y. R. (1993). Vibrational spectroscopy of water at the vapor/water interface. *Physical Review Letters, 70*(15), 2313.

Fakhouri, F. M., Fontes, L. C. B., Gonçalves, P. V. M., Milanez, C. R., Steel, C. J., & Collares-Queiroz, F. P. (2007). Filmes e coberturas comestíveis compostas à base de amidos nativos e gelatina na conservação e aceitação sensorial de uvas crimson. *Ciência e Tecnologia de Alimentos, 27*(2), 369–375.

Famá, L., Flores, S. K., Gerschenson, L., & Goyanes, S. (2006). Physical characterization of cassava starch biofilms with special reference to dynamic mechanical properties at low temperatures. *Carbohydrate Polymers, 66*, 8–15.

Famá, L., Goyanes, S., & Gerschenson, L. (2007). Influence of storage time at room temperature on the physicochemical properties of cassava starch films. *Carbohydrate Polymers, 70*, 265–273.

Famá, L.M., Goyanes, S., Pettarin, V., & Bernal, C.R. (2015). Mechanical behavior of starch-carbon nanotubes composites. In *Handbook of polymer nanocomposites. Processing, performance and application* (pp. 141–171). Berlin Heidelberg: Springer.

Famá, L., Rojas, A. M., Goyanes, S., & Gerschenson, L. (2005). Mechanical properties of tapioca-starch edible films containing sorbates. *Lebensmittel Wissenschaft und Technologie, 38*, 631–639.

Farhat, I. A., Oguntona, T., & Neale, R. J. (1999). Characterisation of starches from West Africa ymas. *Journal of the Science of Food and Agriculture, 79*, 2105–2112.

Fayolle, B., Audouin, L., & Verdu, J. (2000). Oxidation induced embrittlement in polypropylene - a tensile testing study. *Polymer Degradation and Stability, 70*(3), 333–340.

FDA. (2013). US Federal Drug Administration. Code of Federal Regulations 179.41. Pulsed light for the treatment of foods. In: http://www.accessdata.fda.gov/scripts/cdrh/cfdocs/cfcfr/CFRSearch.cfm?CFRPart=179&showFR=1.

Flores, S. K., Famá, L., Rojas, A. M., Goyanes, S., & Gerschenson, L. (2007). Physical properties of tapioca-starch edible films: influence of filmmaking and potassium sorbate. *Food Research International, 40*, 257–265.

García, N. L., Famá, L., Dufresne, A., Aranguren, M., & Goyanes, S. (2009). A comparison between the physico-chemical properties of tuber and cereal starches. *Food Research International, 42*, 976–982.

García, A., Martino, M. N., & Zaritzky, N. E. (2000). Microstructural characterization of plasticized starch-based films. *Starch/Staerke, 52*(4), S118–S124.

García-Tejeda, Y. V., López-González, C., Pérez-Orozco, J. P., Rendón-Villalobos, R., Jiménez-Pérez, A., Flores-Huicochea, E., Solorza-Feria, J., & Bastida, C. A. (2013). Physicochemical and mechanical properties of extruded laminates from native and oxidized banana starch during storage. *LWT - Food Science and Technology, 54*, 447–455.

Gennadios, A., Rhim, J. W., Handa, A., Weller, C. L., & Hanna, M. A. (1998). Ultraviolet radiation affects physical and molecular properties of soy protein films. *Journal of Food Science, 63*(2), 225–228.

Gómez-López, V. M., Ragaert, P., Debevere, J., & Devlieghere, F. (2007). Pulsed light for food decontamination: a review. *Trends in Food Science and Technology, 18*, 464–473.

Gontard, N., Guilbert, S., & Cuq, J. L. (1992). Edible wheat gluten films: influence of the main process variable on film properties using response surface methodology. *Journal of Food Science, 57*(1), 190–195.

Gutiérrez, T. J., Pérez, E., Guzmán, R., Tapia, M. S., & Famá, L. (2014). Functional properties of native and modified by crosslinking, dark-cush-cush yam and cassava starches. *Journal of Polymer and Biopolymer Physics Chemistry, 2*(1), 1–5. doi:10.12691/jpbpc-2-1-1.

Gutiérrez, T. J., Tapia, M. S., Pérez, E., & Famá, L. (2015a). Structural and mechanical properties of edible films made from native and modified cush-cush yam and cassava starch. *Food Hydrocolloids, 45*, 211–217. doi:10.1016/j.foodhyd.2014.11.017.

Gutiérrez, T. J., Morales, N. J., Pérez, E., Tapia, M. S., & Famá, L. (2015b). Physico-chemical properties of edible films derived from native and phosphated cush-cush yam and cassava starches. *Food Packaging and Shelf Life, 3*, 1–8. doi:10.1016/j.fpsl.2014.09.002.

Gutiérrez, T. J., Tapia, M. S., Pérez, E., & Famá, L. (2015c). Edible films based on native and phosphated 80:20 waxy:normal corn starch. *Starch/Stärke, 67*(1–2), 90–97. doi:10.1002/star.201400164.

Hermans, P. H., & Weidinger, A. (1961). On the determination of the crystalline fraction of polyethylenes from X-ray diffraction. *Makromolecular Chemistry, 44*, 24–36.

Hernández, O., Emaldi, U., & Tovar, J. (2008). In vitro digestibility of edible films from various starch sources. *Carbohydrate Polymers, 71*, 648–655.

Hu, G., Chen, J., & Gao, J. (2009). Preparation and characteristics of oxidized potato starch films. *Carbohydrate Polymers, 76*, 291–298.

Huggins, M. L. (1942). The viscosity of dilute solutions of long-chain molecules. IV. Dependence on concentration. *Journal of the American Chemical Society, 64*(11), 2716–2718.

ISO 527-2. (2012). Determination of tensile properties of plastics. In: https://www.iso.org/obp/ui/#iso:std:56046:en.

Ito, M., & Nagai, K. (2007). Analysis of degradation mechanism of plasticized PVC under artificial aging conditions. *Polymer Degradation and Stability, 92*(2), 260–270.

Izquier, A., & Gómez-López, V. M. (2011). Modeling the pulsed light inactivation of microorganisms naturally occurring on vegetable substrates. *Food Microbiology, 28*, 1170–1174.

Karbowiak, T., Debeaufort, F., Champion, D., & Voilley, A. (2006). Wetting properties at the surface of iota-carrageenan-based edible films. *Journal of Colloid and Interface Science, 294*, 400–410.

Kramer, E. O. (1938). Molecular weight of celluloses and cellulose derivates. *Journal of Industrial and Engineering Chemistry, 30*, 1200–1203.

Krishnamurthy, K., Tewari, J. C., Irudayaraj, J., & Demirci, A. (2010). Microscopic and spectroscopic evaluation of inactivation of *Staphylococcus aureus* by pulsed UV light and infrared heating. *Food and Bioprocess Technology, 3*, 93–104.

Kristo, E., & Biliaderis, C. G. (2007). Physical properties of starch nanocrystalreinforced pullulan films. *Carbohydrate Polymers, 68*, 146–158.

Lee, C. Y., McCammon, J. A., & Rossky, P. J. (1984). The structure of liquid water at an extended hydrophobic surface. *The Journal of Chemical Physics, 80*(9), 4448–4455.

Li, M., Liu, P., Zou, W., Yu, L., Xie, F., Pu, H., Liu, H., & Chen, L. (2011). Extrusion processing and characterization of edible starch films with different amylose contents. *Journal of Food Engineering, 106*, 95–101.

MacFarlane, D.S. (Hastings On Hudson, NY), MacFarlane, D.K. (Hastings On Hudson, NY), & Billmeyer, F.W. (Schenectady, NY). (1936). Method and instrument for selecting personal compatible colors. United States Patent 5313267. Available from http://www.freepatentsonline.com/5313267.html.

Manzocco, L., Nicoli, M.C., & Labuza, T. (2003). Study of bread staling by X-ray diffraction analysis. Italian Food Technology, XII, 17–23.

Medina, C., González, P., Goyanes, S., Bernal, C., & Famá, L. (2015). Biofilms based on cassava starch containing extract of yerba mate as antioxidant and plasticizer. *Starch-Starke, 67*(9–10), 780–789.

Merlin, A., & Fouassier, J. P. (1981). Etude de radicaux libres formés par irradiation ultraviolette de l'amidon: application aux ractions de photodegradation et de photogreffage. *Macromolecular Chemistry: Macromolecular Symposium, 182*, 3053–3068.

Miles, M. J., Morris, V. J., & Ring, S. G. (1985a). Gelation of amylose. *Carbohydrate Research, 135*(2), 257–269.

Miles, M. J., Morris, V. J., Orford, P. D., & Ring, S. G. (1985b). The roles of amylose and amylopectin in the gelation and retrogradation of starch. *Carbohydrate Research, 135*(2), 271–281.

Mina, J. H., Valadez, A., Herrera-Franco, P. J., & Toledano, T. (2009). Influencia del tiempo de almacenamiento en las propiedades estructurales de un almidón termoplástico de yuca (TPS). *Ingenieria y Competitividad, 11*(2), 95–106.

Noel, T. R., Ring, S. G., & Whittman, M. A. (1992). The structure and gelatinization of starch: a review. *Food Science Technology Today, 6*, 159.

Ojagh, S. M., Rezaei, M., Razavi, S. H., & Hashem, S. M. (2010). Development and evaluation of a novel biodegradable film made from chitosan and cinnamon essential oil with low affinity toward water. *Food Chemistry, 122*, 161–166.

Osella, C. A., Sánchez, H. D., Carrara, C. R., de la Torre, M. A., & Buera, M. P. (2005). Water redistribution and structural changes of starch during storage of a gluten-free bread. *Starch/Staerke, 57*(5), 208–216.

Otoni, C.G., Avena-Bustillos, R.J., Chiou, B.-S., Bilbao-Sainz, C., Bechtel, P.J., & McHugh, T.H. (2012). Ultraviolet-B radiation induced cross-linking improves physical properties of cold- and warm-water fish gelatin gels and films. *Journal of Food Science,* E1-E9.

Pelissari, F. M., Andrade-Mahecha, M. M., do Amaral, P. J., & Menegalli, F. C. (2013). Comparative study on the properties of flour and starch films of plantain bananas (*Musa paradisiaca*). *Food Hydrocolloids, 30*, 681–690.

Pérez, E., Bahnassay, Y., & Breene, W. (1993). A simple laboratory scale method for isolation of amaranthus starch. *Starch/Staerke, 45*(6), 211–214.

Pérez, E., Gilbert, O., Rolland-Sabaté, A., Jiménez, Y., Sánchez, T., Giraldo, A., Pontoire, B., Guilois, S., Lahon, M.-C., Reynes, M., & Dufour, D. (2010). Physicochemical, functional and macromolecular properties of waxy yam starches discovered from "Mapuey" (*Dioscorea trifida*) genotypes in the Venezuelan Amazon. *Journal of Agricultural and Food Chemistry, 59*(1), 263–273.

Pérez, E., Rolland-Sabaté, A., Dufour, D., Guzmán, R., Tapia, M., Raymundez, M., Ricci, J., Guilois, S., Pontoire, B., Reynes, M., & Gilbert, O. (2013). Isolated starches from yams (*Dioscorea* sp) grown at the Venezuelan Amazons: structure and functional properties. *Carbohydrate Polymers, 98*, 650–658.

Primo-Martin, C., Van Nieuwenhuijzen, N. H., Hamer, R. J., & Van Vliet, T. (2007). Crystallinity changes in wheat starch during the bread-making process: starch crystallinity in the bread crust. *Journal of Cereal Science, 45*, 219–226.

Reyes, L.R. (2013). Caracterización de dispersiones filmogénicas a base de almidón de maíz y ácido oleico en nanoemulsión con capacidad de formación de recubrimientos comestibles activos. Tesis de Maestría. Facultad de Química. Universidad Autónoma de Querétaro. México.

Rhim, J. W., & Wang, L. F. (2013). Mechanical and water barrier properties of agar/kcarrageenan/konjac glucomannan ternary blend biohydrogel films. *Carbohydrate Polymers, 96*, 71–81.

Rhim, J. W., Gennadios, A., Fu, D., Weller, C. L., & Hanna, M. A. (1999). Properties of ultraviolet irradiated protein films. *Lebensmittel-Wissenschaft & Technologie, 32*, 129–133.

Saavedra, N., & Algecira, N. (2010). Evaluación de películas comestibles de almidón de yuca y proteína aislada de soya en la conservación de fresas. *NOVA-Publicación científica en ciencias biomédicas, 8*(14), 171–182 ISSN:1794-2470.

Sionkowska, A., & Płanecka, A. (2013). Surface properties of thin films based on the mixtures of chitosan and silk fibroin. *Journal of Molecular Liquids, 186*, 157–162.

Sionkowska, A., Płanecka, A., Lewandowska, K., & Michalska, M. (2014). The influence of UV-irradiation on thermal and mechanical properties of chitosan and silk fibroin mixtures. *Journal of Photochemistry and Photobiology B: Biology, 140*, 301–305.

Thielemans, W., Belgacem, M. N., & Dufresne, A. (2006). Termoplastic starch-waxy maize starch nanocrystals nanocomposites. *Langmuir, 22*, 4804–4810.

Turton, T. J., & White, J. R. (2001). Degradation depth profiles and fracture of UV exposed polycarbonate. *Plastics, Rubber and Composites, 30*(4), 175–182.

Uesugi, A., & Moraru, C. I. (2009). Reduction of listeria on ready-to-eat sausages after exposure to a combination of pulsed light and nisin. *Journal of Food Protection, 72*(2), 347–353.

Ummi-Shafiqah, M. S., Fazilah, A., Karim, A. A., Kaur, B., & Yusup, Y. (2012). The effects of UV treatment on the properties of sago and mung bean films. *International Food Research Journal, 19*(1), 265–270.

Vaz, C. M., De Graaf, L. A., Reis, R. L., & Cunha, A. M. (2003). Effect of crosslinking, thermal treatment and UV irradiation on the mechanical properties and in vitro degradation behavior of several natural proteins aimed to be used in the biomedical field. *Journal of Materials Science: Materials in Medicine, 14*, 789–796.

Vogler, E. A. (1998). Structure and reactivity of water at biomaterial surfaces. *Advances in Colloid and Interface Science, 74*, 69–117.

Vogler, E. A., Graper, J. C., Harper, G. R., Sugg, H. W., Lander, L. M., & Brittain, W. J. (1995). Contact activation of the plasma coagulation cascade. I. Procoagulant surface chemistry and energy. *Journal of Biomedical Materials Research, 29*(8), 1005–1016.

Wihodo, M., & Moraru, C. I. (2015). Effect of pulsed light treatment on the functional properties of casein films. *LWT–Food Science and Technology, 64*(2), 837–844.

Yoo, S. H., & Jane, J. L. (2002). Molecular weights and gyration radii of amylopectins determined by high-performance size-exclusion chromatography equipped with multi-angle laser-light scattering and refractive index detectors. *Carbohydrate Polymers, 49*(3), 307–314.

Zobel, H.F. (1992). Starch granule structure in: developments in carbohydrate chemistry. In H. F. Zobel and R. J. Alexandes, Edicion A.A.C.C.

Zobel, H. F. (1994). Starch granule structure. In R. J. Alexander & H. F. Zobel (Eds.), *Developments in carbohydrate chemistry* (pp. 1–36). St. Paul, MN: The American Association of Cereal Chemists.

Zobel, H. F., French, A. D., & Hinkle, M. E. (1967). X-ray diffraction of oriented amylose fibers. II. Structure of V amyloses. *Biopolymers, 5*, 837–845.